

# Vitronectin Gene Expression in the Adult Human Retina

Don H. Anderson,<sup>1</sup> Gregory S. Hageman,<sup>2</sup> Robert F. Mullins,<sup>2</sup> Maureen Neitz,<sup>3,4</sup> Jay Neitz,<sup>3,4</sup> Shiro Ozaki,<sup>1</sup> Klaus T. Preissner,<sup>5</sup> and Lincoln V. Johnson<sup>1</sup>

**PURPOSE.** To determine whether vitronectin (Vn), a plasma protein and extracellular matrix molecule that is also a prominent constituent of drusen, is synthesized by cells in the adult human retina.

**METHODS.** The distribution of Vn in the normal adult human retina was examined using antibodies to circulating plasma Vn and to the multimeric, heparin-binding form that is most prevalent in extravascular tissues. Evidence of Vn transcription by retinal cells was analyzed by in situ hybridization and also by reverse transcription of total RNA derived from dissociated human or mouse photoreceptors followed by amplification using polymerase chain reaction (RT-PCR).

**RESULTS.** Cytoplasmic immunoreactivity for plasma Vn or multimeric Vn was detected in photoreceptors, in a subpopulation of neurons situated in the inner retina, and in vitreous hyalocytes. Extracellular labeling was limited primarily to Bruch's membrane and the retinal vasculature. At the transcriptional level, Vn mRNA was localized to both photoreceptors and ganglion cells by in situ hybridization. The in situ findings were corroborated by RT-PCR using total RNA from dissociated mouse or human photoreceptor cells.

**CONCLUSIONS.** The results constitute the first evidence for Vn gene expression by adult neurons in the mammalian central nervous system. The identification of the photoreceptors as a cellular source of Vn suggests that these cells have the potential to make a biosynthetic contribution to the Vn that is found in drusen. (*Invest Ophthalmol Vis Sci.* 1999;40:3305-3315)

Vitronectin (Vn), also known as serum-spreading factor or S-protein, is an adhesive glycoprotein that circulates at high concentration in plasma. It is also a common component of extracellular matrices in adult tissues,<sup>1</sup> including Bruch's membrane.<sup>2</sup> More than 98% of plasma Vn (Vn<sub>p</sub>) circulates in a latent monomeric conformation, whereas much of the Vn present at extravascular sites exists in a reactive, heparin-binding form that tends to self-aggregate into multimeric complexes.<sup>3,4</sup> The conformational change of Vn from the monomeric plasma form to the heparin-binding form appears to be a key event in the functional activation of the molecule.<sup>5</sup>

In addition to its established role in mediating cell adhesion, Vn also has regulatory roles in complement-mediated cell lysis, fibrinolysis, thrombosis, inflammation, and phagocytosis.<sup>6,7</sup> These functions are mediated through its interactions

with a number of different molecules, including membrane receptors (i.e., integrins), terminal complement components, the thrombin-anti-thrombin III complex, and plasminogen activator inhibitor (PAI) -1.

Formerly, Vn was thought to be synthesized exclusively by liver hepatocytes<sup>8</sup>; however, more sensitive assays led to the identification of extrahepatic sites of Vn transcription in murine tissues, with the brain among the most prominent of these extrahepatic sources.<sup>9</sup> Although overall levels of Vn transcripts in murine brain and other organs are low compared with that in the liver, results from in situ hybridization studies in the mouse suggest that the absolute levels of Vn mRNA in hepatocytes and in some brain cells are comparable.<sup>10</sup>

The presence of Vn immunoreactivity (IR) in the plaques and extracellular deposits associated with several age-related diseases has led to speculation about its potential role in the pathogenesis of some of these disorders. For example, Vn is located in the deposits associated with elastotic skin lesions<sup>11</sup> and glomerulonephritis,<sup>12,13</sup> in the plaques characteristic of Alzheimer's disease<sup>14</sup> and atherosclerosis,<sup>15-17</sup> and, most recently, in the abnormal ocular deposits known as drusen<sup>2</sup> that are strongly correlated with age-related macular degeneration.

To improve our understanding of Vn's function in the central nervous system and its potential involvement in neurodegenerative diseases such as age-related macular degeneration, we undertook a study of Vn gene expression and protein distribution in the normal adult human retina. The results provide the first evidence for Vn gene expression by adult neurons and, in particular, by photoreceptor cells and retinal ganglion cells. They also demonstrate that Vn IR is present at intracellular and extracellular retinal sites associated with both neuronal and nonneuronal cell types. Because Vn, like most other plasma proteins, is normally excluded from the retina by the blood-retinal barrier, the synthesis of this molecule by

---

From the <sup>1</sup>Center for the Study of Macular Degeneration, Neuroscience Research Institute, University of California, Santa Barbara; <sup>2</sup>The University of Iowa Center for Macular Degeneration, Iowa City; <sup>3</sup>Department of Cell Biology and Anatomy and <sup>4</sup>The Eye Institute, Medical College of Wisconsin, Milwaukee; <sup>5</sup>Institut für Biochemie, Justus-Liebig-Universität, Giessen, Germany.

Supported by research Grants EY02082 and EY11521 (DHA), EY11515 (GSH), EY11527 (LVJ) from the National Eye Institute (NEI), National Institutes of Health (NIH); NEI Core Grant EY01931 for Vision Research, and an unrestricted grant from Research to Prevent Blindness (RPB) awarded to the Medical College of Wisconsin, Department of Ophthalmology, and a James S. Adams Special Scholar Award (MN) from RPB.

Submitted for publication January 21, 1999; revised April 9 and May 28, 1999; accepted July 14, 1999.

Commercial relations policy: N.

Corresponding author: Don H. Anderson, Center for the Study of Macular Degeneration, Neuroscience Research Institute, University of California, Santa Barbara, CA 93106.

E-mail: d\_anders@lifesci.ucsb.edu

local cell types suggests that one or more elements of its functional repertoire may be required for normal retinal function.

## MATERIALS AND METHODS

### Mammalian Tissues and Cells

**Human Tissues.** Human eyes from 15 individual donors, were obtained from MidAmerica Transplant Services (St. Louis, MO), the Doheny Eye and Tissue Transplant Bank of the Central Coast (Goleta, CA), or the Eye Institute at the Medical College of Wisconsin (Milwaukee). All eyes were processed within 2 to 6 hours of death. After removal of the anterior segments, the posterior poles were examined under a stereomicroscope to confirm the absence of gross retinal disease. In some cases, retinal punches were obtained using a 6-mm trephine. The neural retinas from the punches were peeled away from the retinal pigment epithelium (RPE)-choroid-sclera using fine forceps. For dissociation experiments, retina punches were transferred to an ice bath containing serum-free mammalian cell culture medium (Eagle's minimum essential medium [MEM]; pH 7.1) supplemented with 5% sucrose. Retinal punches from the superior central retinas of four normal adult donors ranging in age from 46 to 54 years were earmarked for end-point reverse transcription-polymerase chain reaction (RT-PCR). These punches were transferred to cryovials, snap frozen immediately in liquid nitrogen, and stored at  $-80^{\circ}\text{C}$ . Samples of normal adult human liver were obtained within 2 hours of biopsy from Harvey Solomon (St. Louis University School of Medicine, MO) and treated similarly. For the transmission light microscopic analyses, the eyes from another three normal donors (ages 33, 53, and 59) were used. For the confocal microscopic analysis, the eyes from six additional donors ranging in age from 42 to 79 years were used. For the dissociation experiments, the photoreceptor slabs were isolated from the eyes of two normal adult donors.

**Dissociated Human Photoreceptors.** Small pieces of the outer retina containing the photoreceptor outer segments and inner segments were gently teased away from the inner retina and harvested using a small-bore glass pipette. Microscopic examination revealed that the harvested slabs fractured uniformly and then resealed at a location just distal to the cell body at the level of the outer limiting membrane. Mild vortexing of the isolated photoreceptor slabs was used to dissociate the cells further into smaller clusters and single photoreceptor fragments that included the outer segment, ellipsoid, and myoid regions. This served as the starting material for the human photoreceptor cell RT-PCR analysis.

**Dissociated Mouse Photoreceptors.** All mice used in this study were treated in accordance with the ARVO Statement for the Care and Use of Animals in Ophthalmic and Vision Research. Mice (C57 B/6) were killed by intraperitoneal injection of an overdose of sodium pentobarbital. Afterward, the globes were enucleated and, after removal of the anterior segment, the posterior segments were placed in ice-cold buffered medium (25 mM HEPES-DMEM, pH 7.4; Life Technologies, Grand Island, NY). Retinae were peeled away from the RPE-choroid using forceps and then placed in a tube containing 1 ml buffered medium. Single photoreceptor cells were dissociated from the remaining retinae by mild vortexing using three, brief 1- to 2-second pulses. Fifty microliters of the pho-

photoreceptor cell suspension was collected, diluted into 1 ml fresh buffered medium, and plated on poly-L-lysine-coated (5  $\mu\text{g}/\text{ml}$ ) glass coverslips. After settling for 30 minutes at  $4^{\circ}\text{C}$ , a coverslip with attached cells was placed in a sealed chamber equipped with inflow and outflow ports. Tubing to the inflow port was connected to a peristaltic pump, and the chamber was mounted onto the stage of an inverted microscope. Coverslips were washed continuously for approximately 30 minutes with buffered medium to remove nonadherent cells, cell debris, and other potential contaminants. After this washing procedure, intact photoreceptors were identified in the microscope and collected by suction using a glass micropipette (5–10- $\mu\text{m}$  tip diameter; Garner Glass, Claremont, CA) mounted in a micromanipulator (Narishige, Tokyo, Japan). For control purposes, an equal volume of chamber medium with no photoreceptors was also collected. Finally, the micropipette tip containing harvested samples was placed into a 0.2-ml PCR tube containing 5.0  $\mu\text{l}$  of 0.1% Triton X-100 (Pierce, Rockford, IL) and the glass tip was fractured on the sidewall of the tube. Specimen tubes were stored at  $-70^{\circ}\text{C}$  for later analysis.

### Antibodies and Molecular Probes

A rabbit polyclonal antibody raised against human  $\text{Vn}_p^{18}$  was used at a dilution of 1:300 from the stock concentration. The antiserum was adsorbed against Vn-depleted human plasma proteins and human fibronectin (Life Technologies). Rabbit anti-bovine Vn, purchased from the same source, was used at a dilution of 1:300 to 1:600 from stock.<sup>18</sup> Vn monoclonal antibody 16A7 was used at a concentration of 5 to 10  $\mu\text{g}/\text{ml}$ . The 16A7 antibody reacts preferentially with the multimeric form of Vn ( $\text{Vn}_m$ ).<sup>4</sup> For immunofluorescence detection, donkey anti-rabbit or donkey anti-mouse IgGs conjugated to indocarbocyanine 2 (Cy2) or indocarbocyanine 3 (Cy3) were used (Jackson ImmunoResearch, West Grove, PA). For frozen and paraffin-embedded tissue, biotin-conjugated goat anti-rabbit or goat anti-mouse IgG secondary antibodies were used (Biotek Solutions, Goleta, CA). Avidin-horseradish peroxidase (Biotek Solutions) was used for detection. Vn sense and antisense probes were prepared using a 1.0-kb double-strand human Vn cDNA (nucleic acids 543-1513; Life Technologies) or a pGEM-4Z vector containing a human Vn cDNA insert (nucleic acids 185-872). Full-length, 1.64-kb bovine opsin cDNA was also used to generate positive control probes.

### Gel Electrophoresis and Immunoblot Analysis

Human sera samples were diluted 1:100 in Laemmli sample buffer (Bio-Rad, Richmond, CA) and separated on a 10% sodium dodecyl sulfate-polyacrylamide gels under reducing conditions. After electrophoresis, the separated proteins were transferred onto nitrocellulose filters using standard wet-transfer procedures. After blocking with skim milk, the blotted filters were incubated for 1 hour in buffer containing the primary antibody at a dilution of 1:1000 from stock. After several buffer rinses, blots were incubated for 0.5 hours in buffer containing a 1:16,000 dilution of goat anti-rabbit IgG-alkaline phosphatase conjugate (Sigma, St. Louis, MO). A detection kit (Bio-Rad) containing 5-bromo-4-chloro-3-indolylphosphate and nitro blue tetrazolium was used to visualize the reaction product, according to the instructions of the supplier.

## Immunohistochemistry

Initially, retinal wedges extending from the optic nerve head to the ora serrata were fixed by immersion in 4% paraformaldehyde in 0.1 M sodium cacodylate buffer (pH 7.1) for several hours. After primary fixation, wedges were transferred to buffer containing 0.4% paraformaldehyde and then stored at 4°C. Three by 5-mm rectangular slabs from the central retina were cut out of the wedges using a razor blade and processed for immunohistochemical analysis in one of three ways: For frozen sections, slabs were snap frozen and embedded in a mixture of 15% sucrose and 7.5% gelatin. Five to 7- $\mu$ m-thick frozen sections were cut using a cryostat. For paraffin sections, specimens were dehydrated, embedded in paraffin, and sectioned to the same thickness with glass knives using an ultramicrotome. Both groups were processed for immunohistochemistry using the method described by Geller et al.<sup>19</sup> All sections were blocked by incubation in a 1:100 dilution of globulin-free bovine serum albumin (Fraction V; Sigma) for 1 hour. Immunoblot analysis confirmed that the bovine serum albumin contained no detectable contaminating bovine Vn. For laser scanning confocal immunofluorescence microscopy, specimens were processed using the method described by Matsumoto and Hale.<sup>20</sup> After processing, vibratome sections were mounted on glass microscope slides in glycerol-containing *N*-propyl-gallate to retard fluorescence quenching, cover-slipped, sealed at the edges, and examined immediately by confocal laser scanning microscopy (model 1024; Bio-Rad).

## RT-PCR Analyses

**End-Point Analysis.** Total RNA was extracted (RNeasy Minikit; Qiagen, Santa Clara, CA). cDNAs were synthesized from 1  $\mu$ g total RNA using oligo (dT)<sub>16</sub> as primer in the presence or absence of reverse transcriptase (Superscript II; Gibco; Gaithersburg, MD) according to the manufacturer's instructions. PCR was then performed with cDNA as a template in the presence of primer pairs derived from the human Vn oligonucleotide sequence.<sup>21</sup> The primer sets were spaced so that the coding regions, to which the primers were complementary, were interrupted by an intron. Two sets of Vn primer pairs were used: Primer pair 1, F1: 5'-CGAGGAGAAAAACA-ATGCCAC-3' and B1: 5'-GAAGCCGTCAGAGATATTTTCG-3'; primer pair 2, F2: 5'-CCTTCACCGACCTCAAGAAC-3' and B2: 5'-GAAGCCGTCAGAGATATTTTCG-3'.

The first primer pair was designed to yield an 832-bp genomic Vn fragment and a 502-bp Vn cDNA. The second primer pair was designed to yield similar fragments of 587 bp and 257 bp, respectively. Each primer was used at a final concentration of 1  $\mu$ M. PCR reagents and enzymes were purchased from Life Technologies and used according to the manufacturer's instructions. The DNA was melted at 94°C for 4 minutes. The reaction was run through 35 cycles at 94°C for 30 seconds, 50°C for 30 seconds, and 72°C for 1 minute. The reactions were iced and run on 1.8% agarose gels containing ethidium bromide for visualization of the PCR products.

**Single-Cell Analysis of Human Photoreceptors.** Total nucleic acid was isolated from harvested human photoreceptor cells using Tri Reagent (Molecular Research Center, Cincinnati, OH), as described previously.<sup>22</sup> The RNA was reverse transcribed, and the Vn cDNAs amplified using an RT-PCR kit (PE Applied Biosystems, Foster City, CA). First-strand cDNA synthesis was primed with random hexamer primers provided

with the kit. Primers for PCR amplification were designed using sequences derived from the nucleotide sequence of human Vn.<sup>23</sup> The upstream primer was derived from nucleotides 216–244; the downstream primer was complementary to nucleotides 858–833; upstream primer: 5'-CAC GGT CTA TGA CGA TGG CGA GGA GGA-3'; downstream primer: 5'-CTC CTG ACT GGG CTG GTG CTG GAA CT-3'.

The primers were designed to yield a 643-bp cDNA fragment. Primer pairs were designed to ensure that the coding regions, to which the primers were complementary, were interrupted by an intron. This ensured, based on the smaller size of the PCR product obtained from retinal tissue, that it derived from cDNA rather than genomic Vn DNA. Genomic DNA was isolated from peripheral blood leukocytes to establish that the fragment amplified from genomic DNA differed in size from the fragment amplified from retinal cDNA. Amplification conditions for each primer pair were optimized by titrating the Mg<sup>2+</sup> and primer concentrations. A wax hot-start PCR protocol was followed (Ampliwax Gems; PE Biosystems). DNA sequence analysis of the PCR products was performed by partial cycle sequencing (PE Biosystems) to verify their identities.

**Single-Cell Analysis of Mouse Photoreceptors.** Total nucleic acid from lysed mouse photoreceptors was used for first-strand cDNA synthesis. Then, 0.5  $\mu$ l of a solution containing 6  $\mu$ M oligo(dT)<sub>16</sub> (Boehringer-Mannheim, Indianapolis, IN) was added to PCR tubes containing 5.5  $\mu$ l of the photoreceptor cell-detergent mixture. The tube mixture was heated to 70°C for 10 minutes and then iced for an additional 5 minutes. Next, 4.5  $\mu$ l of a solution containing the following additional reagents was added to each PCR sample tube to achieve the final concentrations indicated: 50 mM Tris-HCl (pH 8.3), 75 mM KCl, 2.5 mM MgCl<sub>2</sub>, 10 mM dithiothreitol, 0.5 mM each of the four deoxyribonucleotide triphosphates (Boehringer-Mannheim), 20 U RNase inhibitor (Promega, Madison, WI), and 100 U reverse transcriptase (Superscript II RNase H<sup>-</sup>; Life Technologies). The entire 10- $\mu$ l volume was incubated for 50 minutes at 42°C, deactivated by heating at 70°C for 15 minutes, and then stored on ice for subsequent PCR amplification. First-round PCR amplification was performed in sample tubes containing 10  $\mu$ l of cDNA template, the outside primer pair derived from the mouse Vn nucleotide sequence,<sup>8</sup> and three additional sets of control primers designed to amplify target sequences from the coding regions of the following genes (see Table 1): phosducin,<sup>21</sup> a phototransduction protein and regulator of G-protein function in photoreceptors that also appears to be expressed in liver, lung, heart, and brain<sup>22</sup>; Thy-1,<sup>24</sup> a cell-surface protein expressed by neurons including retinal ganglion cells, hematopoietic stem cells,<sup>25</sup> and hepatic oval cells<sup>26</sup>; glial fibrillary acidic protein (GFAP),<sup>27</sup> an intermediate filament protein expressed by glia in the brain, in the retina and also by Ito cells in the liver.<sup>28</sup> Next, 40  $\mu$ l of a solution that included the following additional reagents was added to the sample tubes to achieve final concentrations of: 10 mM Tris-HCl (pH 8.3), 50 mM KCl, 2.0 mM MgCl<sub>2</sub>, 0.2 mM each of the four deoxyribonucleotide triphosphates, and 2.5 U *Taq* polymerase (Promega, Madison, WI). Final primer concentration was 0.2  $\mu$ M. Autoclaved, double-distilled H<sub>2</sub>O without reverse transcriptase was included as a negative control. First-round PCR amplification was carried through 40 cycles (94°C, 30 seconds; 55°C, 30 seconds; 72°C, 90 seconds) using a thermal cycler (GeneAmp PCR System 9600; PE Biosystems).

**TABLE 1.** Primer Pairs Derived from Mouse Oligonucleotide Sequences Used for Single-Cell RT-PCR

Vitronectin	
Outside primer pair	F1: 5'-TGCTATGAGCTAGATGAGACG GC-3' B1: 5'-TGAATTGGGGTTCTCTGGCTC-3'
Inside primer pair	F2: 5'-CCAAGATGTCTGGGGCATTG-3' B2: 5'-AGGATCTGCCCCAGAAGAGG-3'
Phosducin	
Outside primer pair	F1: 5'-ACACACACAGGACCCAAA G-3' B1: 5'-CATTTAGGAAAGACTCCACAT C-3'
Inside primer pair	F2: 5'-AGCAGAAAAGATGAGCATTCAAGAATATG-3' B2: 5'-TGCTTATGAGTTCCCCACCTTTG-3'
Glial fibrillary acidic protein	
Outside primer pair	F1: 5'-ATGGAGCTCAATGACCGCTTTGC-3' B1: 5'-CTGTGAGGTCTGGCTTGGCCAC-3'
Inside primer pair	F2: 5'-GAACAGCAAAACAAGGCGCTGGC-3' B2: 5'-AACTGGATCTCCTCCTCCAGCGA-3'
Thy-1	
Outside primer pair	F1: 5'-GTGACCAGCCTGACAGCCTG-3' B1: 5'-CAGAGAAATGAAGTCCAGGGCTG-3'
Inside primer pair	F2: 5'-CAAAACCTTGCCTGGACTGC-3' B2: 5'-CAGCAGCATCCAGGATGTGTCTG-3'

Five microliters of the first-round PCR amplification products were then diluted in 245  $\mu$ l purified H<sub>2</sub>O. Five microliters of the diluted first-round product was placed in new PCR tubes for the second round of amplification, which took place in a final volume of 20  $\mu$ l containing 0.1  $\mu$ M of one of the four inside primer pairs, 0.2 mM each of the four deoxyribonucleotide triphosphates, 20 mM Tris-HCl (pH 8.4), 50 mM KCl, 2.5 mM MgCl<sub>2</sub>, and 2.5 U of *Taq* polymerase (Platinum *Taq*; Life Technologies). Forty second-round PCR cycles (94°C, 30 seconds; 55°C, 30 seconds; 72°C, 90 seconds) were then per-

formed. PCR products were visualized on 1.8% agarose gels, using 7.5  $\mu$ l of final PCR product, and stained with ethidium bromide.

### In Situ Hybridization

**Riboprobe Formation.** Human Vn and bovine opsin cDNAs were subcloned into the Bluescript plasmid (Stratagene, La Jolla, CA). Orientation of the insert was determined by diagnostic restriction enzyme digests. To generate the riboprobe, 10  $\mu$ g of plasmid-insert DNA was linearized by restric-

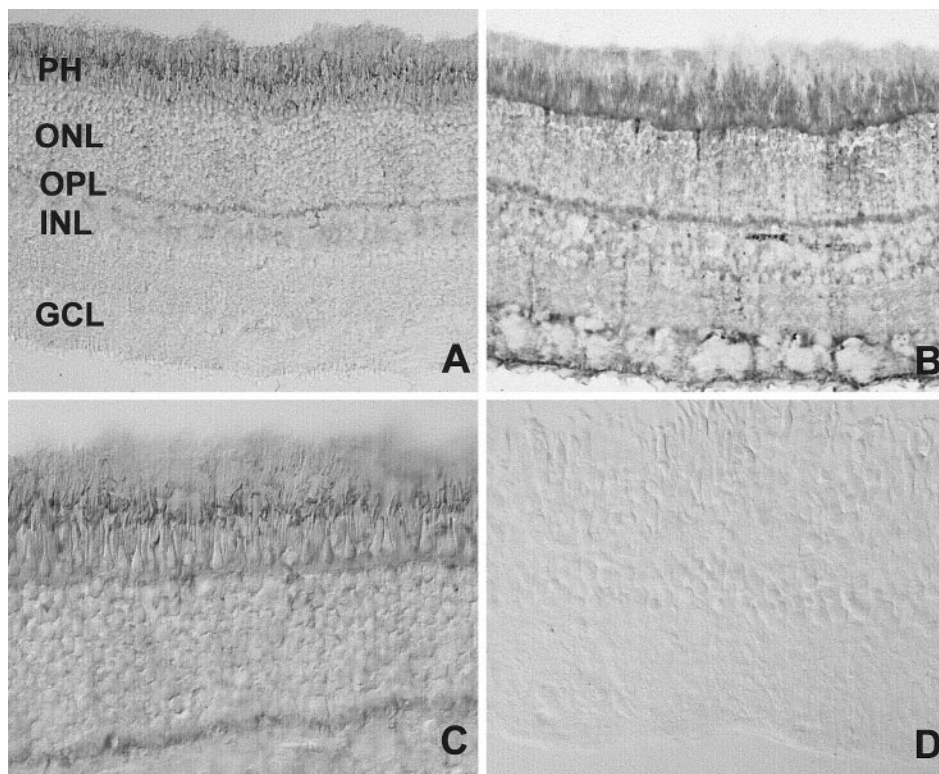
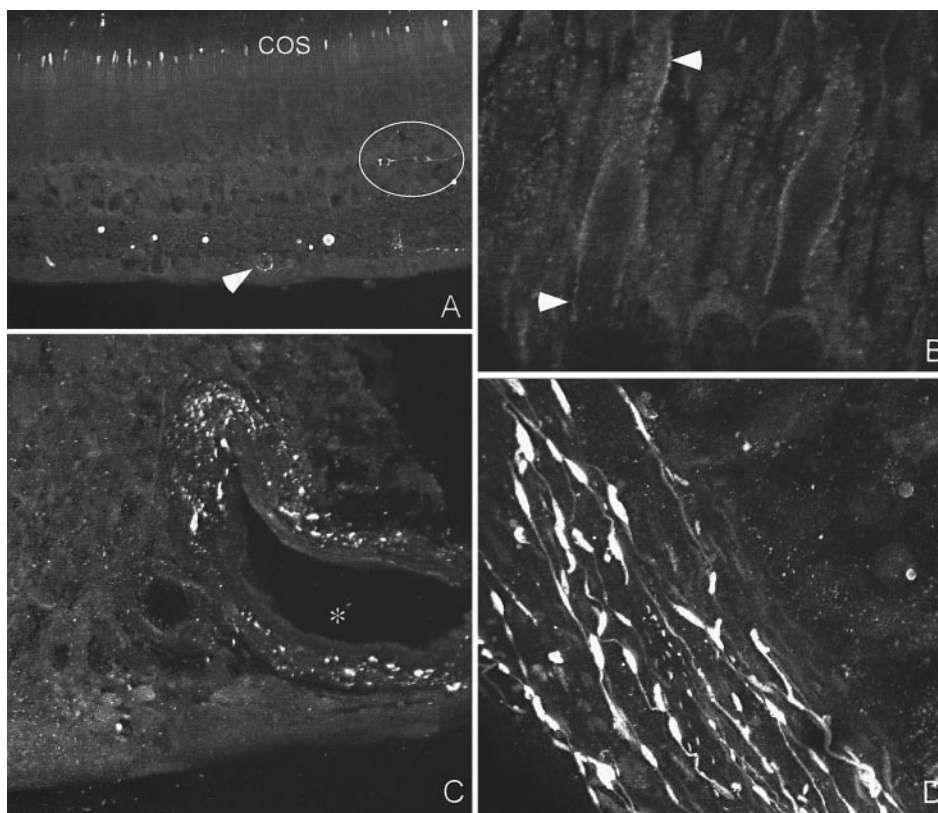


**FIGURE 1.** Vn immunoreactivity in adult human and bovine retinas. Light micrographs of paraformaldehyde-fixed, frozen sections incubated with Vn polyclonal antiserum. (A) Adult human retina. Sections incubated with rabbit anti-human Vn show weak to moderate labeling associated with photoreceptor inner and outer segments (PH). In addition, a thin band of labeling is apparent in the outer plexiform layer (OPL). (B) Bovine retina. Sections incubated with rabbit anti-bovine Vn show a pattern highly similar, but not identical, to the human labeling pattern (see A). In addition to the photoreceptor and OPL labeling, some evidence of Müller cell labeling is evident. (C, D) Specificity of Vn immunolabeling in the adult human retina. (C) Higher magnification of frozen section incubated with Vn polyclonal antiserum as shown in (A). (D) Immunolabeling is blocked when the primary Vn antibody is pre-incubated with 100  $\mu$ g/ml purified human Vn. ONL, outer nuclear layer; INL, inner nuclear layer; GCL, ganglion cell layer. Magnification, (A, D)  $\times$ 256; (B)  $\times$ 240; (C)  $\times$ 460.

**FIGURE 2.** Vn immunoreactivity in the human retina visualized by laser scanning confocal immunofluorescence microscopy. (A) Low-magnification projection series showing labeling of cone outer segments (COS) as well as cell profiles in the OPL (circle) and GCL (arrowhead). (B) In single optical sections, the photoreceptor labeling can be resolved on the cell surfaces of cone inner and outer segments (arrowheads). (C) In this projection series, punctate sub-endothelial labeling is associated with the profiles of retinal vessels (\*). (D) En face view of labeled cells at the vitreoretinal interface. This projection series of 25 1- $\mu$ m images shows a population of anti-Vn positive cells with the morphologic features of hyalocytes, the resident cell type of the vitreous humor. Magnification, (A)  $\times 125$ ; (B)  $\times 2100$ ; (C)  $\times 250$ ; (D)  $\times 165$ .



tion enzyme digest. The linearized DNA was purified by phenol-chloroform extraction followed by gel electrophoresis to verify linearity. The linearized plasmid-insert DNA was cut out of the gel, eluted by centrifugation through glass wool in a microfuge, and further purified using a G-50 Sephadex spin column. The DNA was then precipitated and resuspended. Purified linear DNA (1.5  $\mu$ g) was used as the template for making digoxigenin-labeled riboprobes. The template DNA was incubated for two hours, at 37°C, in a 30- $\mu$ l reaction mix containing 1 $\times$  transcription buffer (Promega), 75 U RNase inhibitor (RNasin; Promega), 100 mM dithiothreitol, digoxigenin RNA-NTP mix (Boehringer-Mannheim), and the appropriate RNA T3 or T7 polymerase (Promega). Integrity of the probe was checked by formaldehyde-agarose gel electrophoresis. To reduce probe size, 15  $\mu$ l diethyl procarbonate-treated H<sub>2</sub>O and 25  $\mu$ l 2 $\times$  carbonate buffer (120 mM Na<sub>2</sub>CO<sub>3</sub> and 80 mM NaHCO<sub>3</sub>) was added to the solution containing the probe and incubated at 65°C for 40 minutes. Ten microliters 20-mg/ml stock of tRNA was then added as a carrier, and the probe was precipitated with LiCl and EtOH, washed with cold 70% EtOH (in diethyl procarbonate-treated H<sub>2</sub>O), dried, and resuspended in DEPC-treated H<sub>2</sub>O.

**Hybridization Protocol.** The performance and specificity of the antisense and sense versions of each probe were evaluated on formaldehyde-fixed, frozen sections of adult human retina using the following parameters: probe concentrations ranging from 0.25 to 3.0  $\mu$ g/ml; hybridization conditions including overnight incubation at 55°C in a probe diluent containing 50% formamide, 5 $\times$  Denhardt's reagent, 0.1% sodium dodecyl sulfate, 5 $\times$  SSPE, 100  $\mu$ g/ml Herring sperm DNA, and diethyl carbonate-treated H<sub>2</sub>O (Biotek Solutions); protein digestion using proteinase K coupled with high stringency

washing conditions (65°C in 0.1 $\times$  SSC for 30 minutes); and detection using a mouse Fab anti-digoxigenin-alkaline phosphatase conjugate (1:200 dilution from stock; Biotek Solutions) and a 5-bromo-4-chloro-3-indolylphosphate-nitro blue tetrazolium chromogenic substrate kit (Vector; Burlingame, CA) to visualize reaction product.

## RESULTS

### Plasma Vn Immunoreactivity in Adult Human and Bovine Retinas

We characterized the Vn<sub>p</sub> antibody on immunoblots of human serum proteins separated on 10.0% polyacrylamide gels. Under reducing conditions, the probe recognized a 65–75-kDa doublet characteristic of Vn<sup>7</sup> (data not shown). When formaldehyde-fixed, frozen sections of adult human retina were probed with the same antibody, photoreceptors displayed some IR, principally at the level of the outer segments. A thin band of labeling was also apparent at the level of the outer plexiform layer (OPL), and traces of extracellular labeling were also noted in the outer nuclear layer (ONL; Figs. 1A, 1C). No labeling was observed in the inner retina (Fig. 1A). Frozen sections of bovine retina that were fixed and processed identically but probed with a polyclonal antibody to bovine Vn showed a similar overall labeling pattern (Fig. 1B). In addition, however, the bovine sections showed evidence of Müller cell labeling, extending from the endfeet at the vitreoretinal border to the outer limiting membrane. The Vn<sub>p</sub> IR in the outer human retina (Fig. 1C) was blocked when the primary anti-Vn<sub>p</sub> antibody was preincubated with purified human Vn (100  $\mu$ g/ml; Fig. 1D).

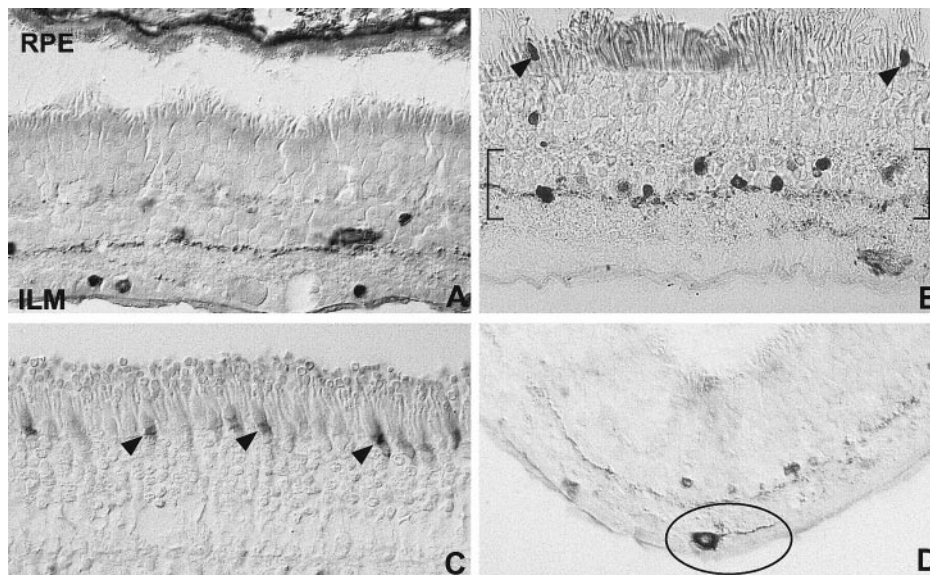


**FIGURE 3.** Immunolocalization of multimeric Vn in the adult human retina. Light micrographs of paraformaldehyde-fixed frozen sections using monoclonal antibody 16A7. (A) Photoreceptor cell labeling is absent. However, there are a number of labeled cell bodies in both the INL and GCL. Bruch's membrane and the inner limiting membrane (ILM) are also labeled. (B) Most of the labeled cells in the inner retina lie within a stratum at the proximal margin of the inner nuclear layer (brackets); some cone myoids are also labeled (arrowheads). (C) In paraffin-embedded tissues, 16A7 immunoreactivity is identified in the myoid region of cone photoreceptor inner segments (arrows). (D) In this frozen section, one of the labeled cell bodies (encircled) is identified as a ganglion cell by its size, location, and associated process. RPE, retinal pigmented epithelium. Magnification, (A)  $\times 240$ ; (B)  $\times 250$ ; (C)  $\times 670$ ; (D)  $\times 400$ .

Several additional features of Vn<sub>p</sub> immunolabeling became apparent in human retinas prepared for confocal immunofluorescence microscopy. Under these conditions, most of the photoreceptor labeling was associated with cones (Fig. 2A). At high magnification, cell surface labeling extended from the distal outer segment to the cone myoid (Fig. 2B). A few labeled cell profiles in the OPL and ganglion cell layer (GCL) were also identified in most sections (Fig. 2A). In those sections where larger retinal vessels were present, punctate subendothelial labeling was clearly evident on the vascular perimeter (Fig. 2C). At the vitreoretinal border, a population of spindle-shaped cell bodies with long, thin bipolar processes was identified (Fig. 2D). These cells have the morphologic characteristics of hyalocytes, the resident cells of the vitreous humor.

#### Immunolocalization of Multimeric Vn in Adult Human Retina

Because the multimerized form of Vn is predominant in the extracellular matrices of many tissues, we examined the distribution of Vn<sub>m</sub> in the retina using a conformation-specific monoclonal antibody (16A7) that recognizes Vn<sub>m</sub> preferentially<sup>4</sup> and whose target epitope lies within a heparin-binding domain of Vn. Using this antibody, the number and location of labeled retinal cells in the human retina was very different from the pattern revealed by the Vn<sub>p</sub> antibody. Photoreceptor labeling was either absent entirely (Fig. 3A) or limited to a small number of cones where it was concentrated in the myoid region of the cell (Figs. 3B, 3C). In contrast to the Vn<sub>p</sub> pattern, there was also a stratum of labeled cells in the inner retina located at the border of the inner nuclear and inner plexiform layers (Figs. 3A, 3B). A number of labeled ganglion cell bodies

were also present (Fig. 3D). Bruch's membrane was heavily labeled, as was the inner limiting membrane in some sections (Fig. 3A).

#### Analysis of Vn Gene Expression in the Adult Human Retina

End-point RT-PCR analyses of total RNA obtained from normal adult human retinas suggested that at least some of the Vn detected immunocytochemically may have originated from one or more local cellular sources within the neural retina. Primer set 1 amplified a cDNA product of 502 bp that corresponds to Vn mRNA (Fig. 4, top; lanes 1 through 4). As expected, the same 502-bp amplicon was also detected in RNA isolated from adult human liver. In the absence of reverse transcriptase, only the larger 832-bp genomic product was apparent (data not shown). Similar results were obtained with the second set of primers (Fig. 4, bottom). The second Vn primer pair amplified a 257-bp product representing Vn mRNA.

#### Localization of Vn Transcripts in Photoreceptors and Ganglion Cells

In situ hybridization data obtained using two different digoxigenin-labeled Vn cRNA antisense probes were consistent with both the RT-PCR and immunocytochemical findings. In the parafoveal retina, the Vn antisense riboprobe hybridized to photoreceptor inner segments and to cell bodies in both the ONL and GCL; (Fig. 5A); the Vn sense version produced no labeling above background levels (Fig. 5B). At higher magnification, antisense labeling of cone photoreceptor inner segments as well as cone cell bodies could be visualized (Fig. 5C).

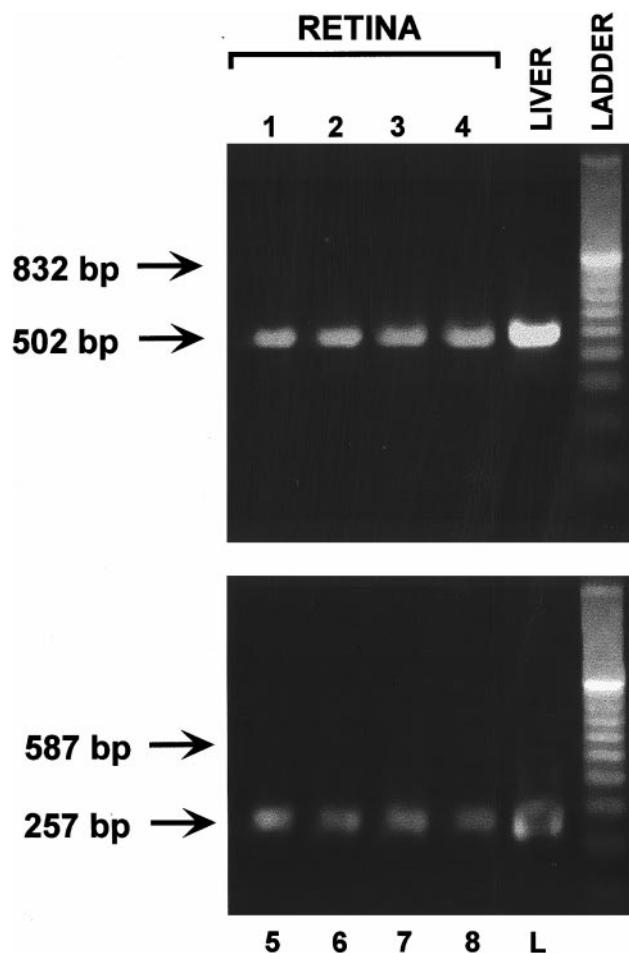


**FIGURE 4.** Identification of Vn-derived PCR products in adult human retina by RT-PCR. Agarose gel (1.8%) stained with ethidium bromide illustrates RT-PCR products amplified from total RNA obtained from four adult human donors (lanes 1 through 4). Total RNA obtained from human liver was used as a positive control. The two predicted genomic fragments (832 bp: arrow, top; 587 bp: arrow, bottom) are not detected under these conditions. The 502- and 257-bp amplicons (arrows) representing Vn mRNA are present in each of the four donor retinas as well as the liver control.

Labeling of the GCL was restricted to cell bodies. A few cells in the proximal portion of the inner nuclear layer, in the inner plexiform layer, and in the vessel wall also showed labeling above background levels (Fig. 5D). There was no evidence of hybridization to the RPE, astrocytes, or Müller cells. Both positive and negative controls using sense and antisense opsin riboprobes yielded the expected results. The opsin antisense probe produced an intense bimodal concentration of reaction product in rod photoreceptor inner segments and rod cell bodies located in the ONL (Fig. 5E). No hybridization occurred using the sense version of the opsin probe (Fig. 5F).

#### Evidence of Vn Transcription by Dissociated Human Photoreceptor Cells

RT-PCR analyses of dissociated human photoreceptor cell clusters also suggested that these cells are a local cellular source of Vn. In the photoreceptor cell-enriched material and in RNAs obtained from extracts of total retina or residual inner retina,

two amplicons were detected (Fig. 6). The larger of the two was a 1076-bp genomic Vn component based on the size of a similar fragment amplified from the nucleic acid fraction of peripheral blood leukocytes (data not shown). DNA sequence analysis confirmed the second smaller 643-bp product (Fig. 6, lanes 2 through 5) as human Vn cDNA derived from the appropriate region. Interestingly, this product was not detected in material obtained from the peripheral rod-rich "patch" under these conditions (lane 1). However, it was detected in the cone-rich foveal material (lane 2) and in the inner retina (lanes 3 and 4). A third, slightly smaller component was also identified in the cone-rich and inner retina fractions. DNA sequencing of this band showed it to be a human Vn sequence without a 166-bp fragment (nucleotides 641–805) that codes for amino acids 205–259, a region that includes the latter part of the first hemopexin domain.

#### Evidence of Vn Transcription in Single Mouse Photoreceptors

To determine whether Vn transcripts could be detected in the photoreceptors of mammals other than humans, single photoreceptors were harvested from adult mice by suction using a glass micropipette, and the nucleic acid fraction was analyzed by single-cell RT-PCR using primers derived from the nucleotide sequence of mouse Vn. As shown in Figure 7, a single fragment of the predicted size (389 bp) was amplified from the mouse photoreceptor-derived material (lane 1). As expected, the phosducin-positive control primers produced a slightly larger fragment (394 bp; lane 2), and the two negative control primers (Thy-1 and GFAP) produced no amplicons (lanes 3 and 4). When total RNA derived from mouse retina (lanes 5 through 8), mouse brain (lanes 9 through 12), or mouse liver (lanes 13 through 16) was used as a template, PCR products of the appropriate size were amplified by each primer pair. In the absence of photoreceptor-derived template (lanes 17 through 20) or in tubes containing H<sub>2</sub>O only (lanes 21 through 24), no products were detected.

#### DISCUSSION

To our knowledge, the results obtained in this study provide the first evidence for Vn gene expression by adult neurons in the mammalian central nervous system. At the transcriptional level, end-point and quantitative RT-PCR analyses indicate that the adult human retina is an abundant source of Vn mRNA.<sup>29</sup> The *in situ* hybridization findings point to photoreceptors and retinal ganglion cells as the most likely cellular sources of Vn in the human retina. No evidence of hybridization is detected in astrocytes or Müller cells. The detection of Vn-derived amplicons in RNA isolated from photoreceptors harvested from the fovea and the failure to detect such amplicons in rod-rich extrafoveal material suggests that cones rather than rods may be the source of Vn mRNA in human photoreceptors. However, detection of Vn mRNA in single photoreceptors harvested from the rod-dominant mouse retina suggests that rods cannot be eliminated as a source of Vn transcripts, at least in this species.

Although Vn is expressed by cells of neuronal origin in the normal adult retina, evidence for expression of Vn at other locations in the nervous system is sparse. Vn transcripts are not detected in mouse brain neurons or vascular endothelial cells

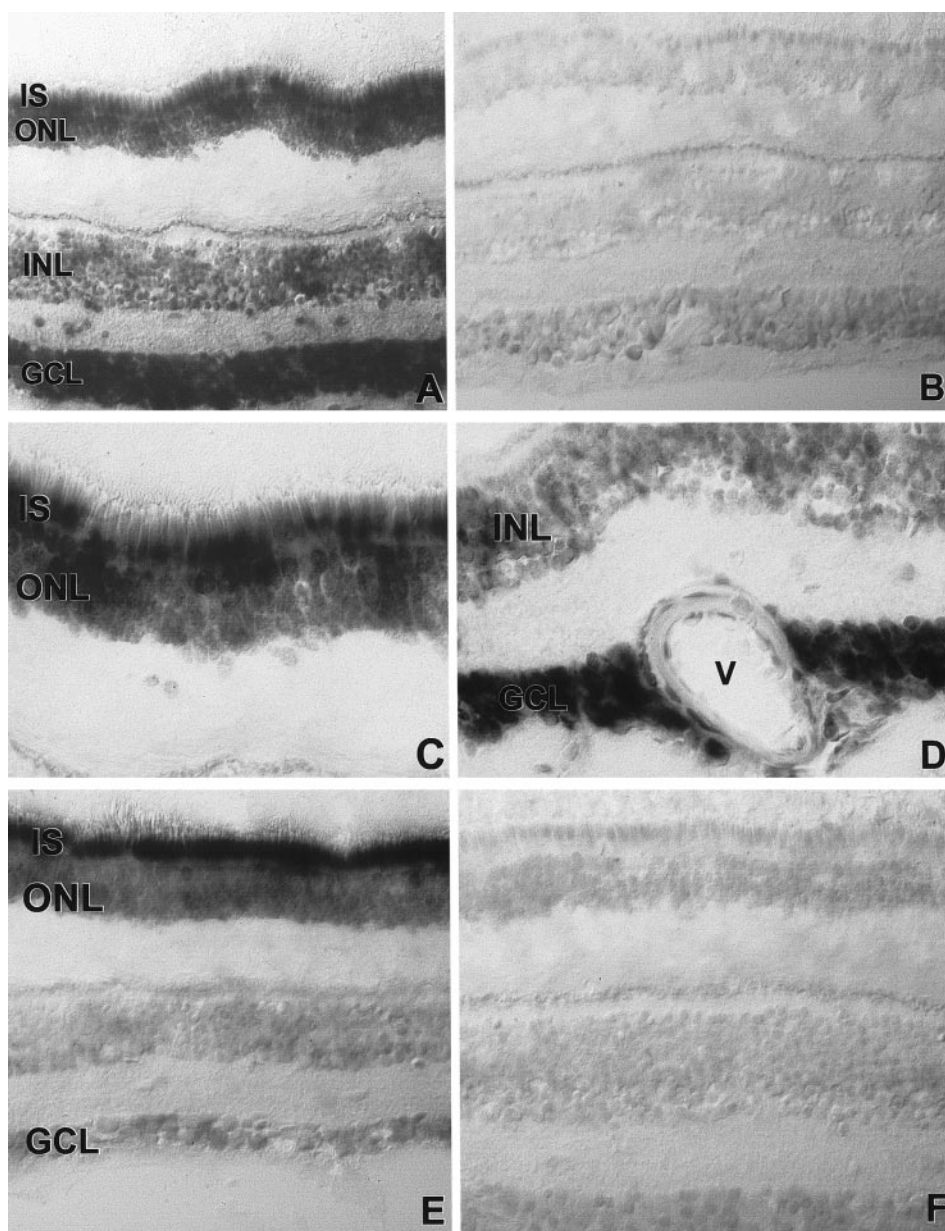


**FIGURE 5.** Localization of Vn transcripts in adult human retina by in situ hybridization. (A) Frozen sections of central retina probed with digoxigenin-labeled Vn antisense probe and detected with anti-digoxigenin-5-bromo-4-chloro-3-indolylphosphate. The probe hybridizes to photoreceptor inner segments (IS) and cell bodies in the ONL. Strong hybridization is also present in the GCL. (B) No hybridization is evident when the Vn sense probe is substituted for the antisense probe. (C) Higher magnification of the Vn antisense hybridization in a cone-rich region of the central retina. (D) High-magnification view of Vn antisense hybridization in the ganglion cell layer (GCL) taken from the same region. Ganglion cell bodies are labeled, and at least two perivascular cells in the vessel wall appear to be above background levels. Retinal vessel (V). (E) Positive control using opsin antisense. Opsin transcripts are localized to photoreceptor inner segments and cell bodies in the outer nuclear layer (ONL). (F) Negative control using opsin sense probe. No hybridization is evident in any of the retinal layers. Magnification, (A, B)  $\times 240$ ; (C)  $\times 450$ ; (D)  $\times 380$ ; (E)  $\times 300$ ; (F)  $\times 260$ .

by in situ hybridization; instead, most labeled cells appear to be associated with the meninges or are near small capillaries.<sup>10</sup> The absence of GFAP IR in these cells seems to rule out astrocytes as a source of Vn in normal brain. In contrast, Vn IR is found in reactive astrocytes and dystrophic axons located in human multiple sclerotic lesions.<sup>30</sup> In the developing chick retina, Vn transcripts and Vn IR are localized to the neuronal layers, and Vn IR is found throughout the retinal extracellular matrix.<sup>30,31</sup> Finally, evidence of Vn transcription and IR is also associated with developing neurons in the ventral region of the neural tube.<sup>32</sup> Some of these differences may be accounted for by species differences, the use of different techniques, or the presence or absence of disease, as has recently been reported in the retinas of normal adult and diabetic rats.<sup>33</sup>

Our immunolocalization results lend additional support to the conclusion that some neurons in the human retina are local biosynthetic sources of Vn. Vn IR is found most consistently in human cones, as well as in a subpopulation of cells with

neuronal morphology located in the OPL, inner nuclear layer, and GCL. Labeling in rods is much less convincing (Figs. 1A, 1C). In other mammals, however, this pattern is not as clear cut. In bovine retina, photoreceptor labeling does not appear to be restricted solely to cones (Fig. 1B) and in rat retinas probed with anti-rat Vn, intense labeling of cones is accompanied by less intense cell surface labeling of rod outer segments (Ozaki and Anderson, unpublished observations).

In human cones, the cell surfaces of both inner and outer segments are labeled using a plasma Vn polyclonal antibody, whereas the intracellular labeling generated by the 16A7 monoclonal antibody that recognizes Vn<sub>m</sub> is concentrated in the myoid region where most of the cells' biosynthetic organelles are compartmentalized. The explanation for this difference is not apparent. One possibility is that the epitope recognized by 16A7 is exposed or more accessible during biosynthesis of the protein. In other retinal neurons, most of the Vn<sub>m</sub> IR also appears to be cytoplasmic. It is also possible that a portion of

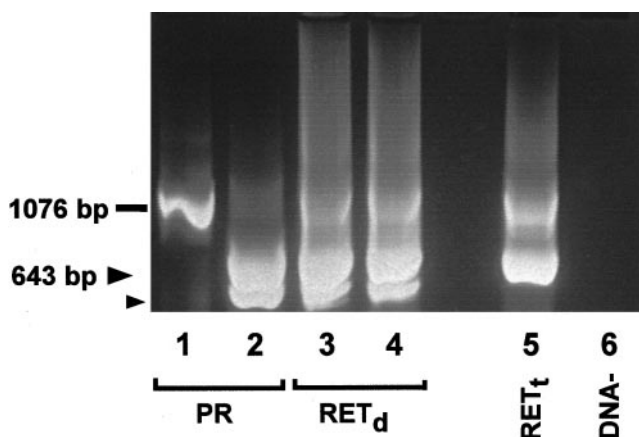


**FIGURE 6.** Identification of Vn amplicons in dissociated human photoreceptors. Ethidium bromide stained gel (2% agarose) of RT-PCR products obtained using cDNA template derived from the nucleic acid fraction of human photoreceptors (PR). *Lane 1:* peripheral, rod-rich fraction. A single 1076-bp fragment (*bar*) representing genomic Vn is amplified under these conditions. *Lane 2:* foveal photoreceptor cell cluster. A 643-bp cDNA representing Vn mRNA is detected (*large arrowhead*), and a third slightly smaller fragment is also apparent (*small arrowhead*). Sequence analysis of this smaller product in *lane 2* showed that it is identical with the larger fragment, except that it contains a 166-bp deletion corresponding to nucleotides 641–805. *Lanes 3 and 4:* residual retina without photoreceptor layer (RET<sub>d</sub>). *Lane 5:* total retina (RET<sub>t</sub>). *Lane 6:* no template control (DNA–).

the Vn<sub>p</sub> labeling is due to cross-reactivity with a putative human counterpart to nectinepsin, an avian gene with substantial sequence homology to human Vn, that has been described in quail retina.<sup>31</sup>

Although the results from this study strongly suggest that Vn is expressed by at least two classes of retinal neurons, the functional significance of these results is unknown. The liver is the primary source of most plasma proteins and it is therefore unclear why Vn biosynthesis occurs in the retina, particularly in photoreceptors. However, there is evidence that several other plasma proteins including transferrin,<sup>32</sup> haptoglobin, and hemopexin<sup>34</sup> are also synthesized by photoreceptors. These proteins are functionally related by their ability to protect cells from oxidative damage, and it has been proposed that retinal biosynthesis is required because access to these molecules' protective effects is denied by the blood-retina barrier.<sup>34</sup> A similar argument can be advanced for Vn, which is also regarded as a multifunctional host protection factor by virtue of its ability to modulate pericellular proteolysis, stabilize cell-extracellular matrix interactions<sup>35</sup> and prevent complement-mediated cell lysis.<sup>36</sup>

Vn also plays a prominent role in nonimmune-mediated phagocytosis of cells, bacteria, and particulates by alveolar macrophages. In vitro and in vivo assays show that preincubation with Vn, arginine-glycine-aspartic acid (RGD)-, or gly-pen-gly-arg-gly-asp-ser-pro-cys-ala (GPeN)-containing peptides significantly improves the efficiency of phagocytosis, whereas Vn receptor blockade inhibits it.<sup>37,38</sup> Vn has also been shown to mediate the phagocytosis of cells undergoing apoptosis by macrophages.<sup>39</sup> The RPE cells, similar to macrophages, are often touted as professional phagocytes because they specialize in the binding, engulfment, and enzymatic digestion of membrane packets shed from the tips of rod and cone outer

segments.<sup>40</sup> Several adhesion-related molecules have been advanced as putative phagocytosis receptors.<sup>41,42</sup> Most recently, this list has been broadened to include a Vn receptor ( $\alpha v\beta 5$ ) located on the apical surface of the RPE.<sup>43,44</sup> Experimental studies in cultured cells suggest that Vn, in concert with  $\alpha v\beta 5$ , may be involved in the binding phase of photoreceptor outer segment phagocytosis by the RPE.<sup>44–46</sup> The results from the current study strongly suggest that cones are a source of Vn in the human retina, but the evidence for expression by rods is weak. If Vn participates in some manner in the phagocytosis of outer segments, a more widespread distribution of Vn IR in the interphotoreceptor matrix and evidence of Vn mRNA in human rods, as well as in mouse rods, might be expected. Additional in situ hybridization studies and quantitative RT-PCR studies focusing on regional differences in the levels of Vn gene expression in the human retina should help to resolve this question.

Vn has now been identified as a ubiquitous component of both hard and soft drusen: the age-related extracellular deposits associated with Bruch's membrane.<sup>2</sup> Although many hypotheses of drusen formation have been advanced since the beginning of this century, their origin has never been firmly established, and their composition remains poorly characterized. Because Vn is synthesized primarily in the liver and is found in such high concentration in plasma, the retinal and/or choroidal circulation could well be a source of Vn that selectively accumulates in drusen. Tight junctions between the endothelial cells of retinal capillaries normally do not allow extravasation of plasma proteins.<sup>47</sup> Similarly, choroidal capillaries appear to curtail the extravasation of molecules with Stoke's radii ( $R_s$ ) greater than serum albumin ( $R_s = 3.5$  nm),<sup>48</sup> such as Vn<sub>p</sub> ( $R_s = 3.9$  nm) and Vn<sub>m</sub> ( $R_s = 5.6$  nm).<sup>3</sup> In aged or diseased retinas, however, such diffusion barriers could be compromised,<sup>49</sup> thereby allowing access of plasma proteins such as Vn to potential sites of drusen formation along Bruch's membrane. Further study of the RPE-choroid in fetal and very young tissues should help clarify whether the deposition of Vn along Bruch's membrane is an age-related phenomenon, as it has been shown to be in the skin,<sup>11</sup> or whether it should be viewed as a normal component of Bruch's membrane.

Translocation of intact Vn from the luminal surface of endothelial cells to the subcellular matrix has been reported,<sup>50</sup> and it has been suggested that such a mechanism could account for the accumulation of Vn in atherosclerotic plaques. By analogy, translocation of plasma Vn across the choroidal endothelium or across the RPE can also be considered possible transcellular pathways for Vn deposition in drusen.

Retinal and/or choroidal vascular cells could be a source of the Vn in drusen. The anti-Vn IR identified in profiles of retinal vessels and in the choriocapillaris is particularly suggestive in that regard. Robust levels of Vn IR are also associated with both the normal and atherosclerotic vascular wall,<sup>51</sup> but evidence of Vn biosynthesis by vascular cells is extremely sparse. In one study, Vn mRNA is reportedly localized to fibrotic regions of the aorta in hyperlipidemic rabbits,<sup>48</sup> but similar evidence of Vn transcription by endothelial or other perivascular cells was not confirmed in subsequent studies.<sup>10,51</sup>

Finally, the RPE is also a logical candidate for a local cellular source of Vn in drusen. We have recently reported evidence of Vn transcription in the human RPE-choroid and in cultured human RPE cells using the RT-PCR.<sup>2,29</sup> However, no

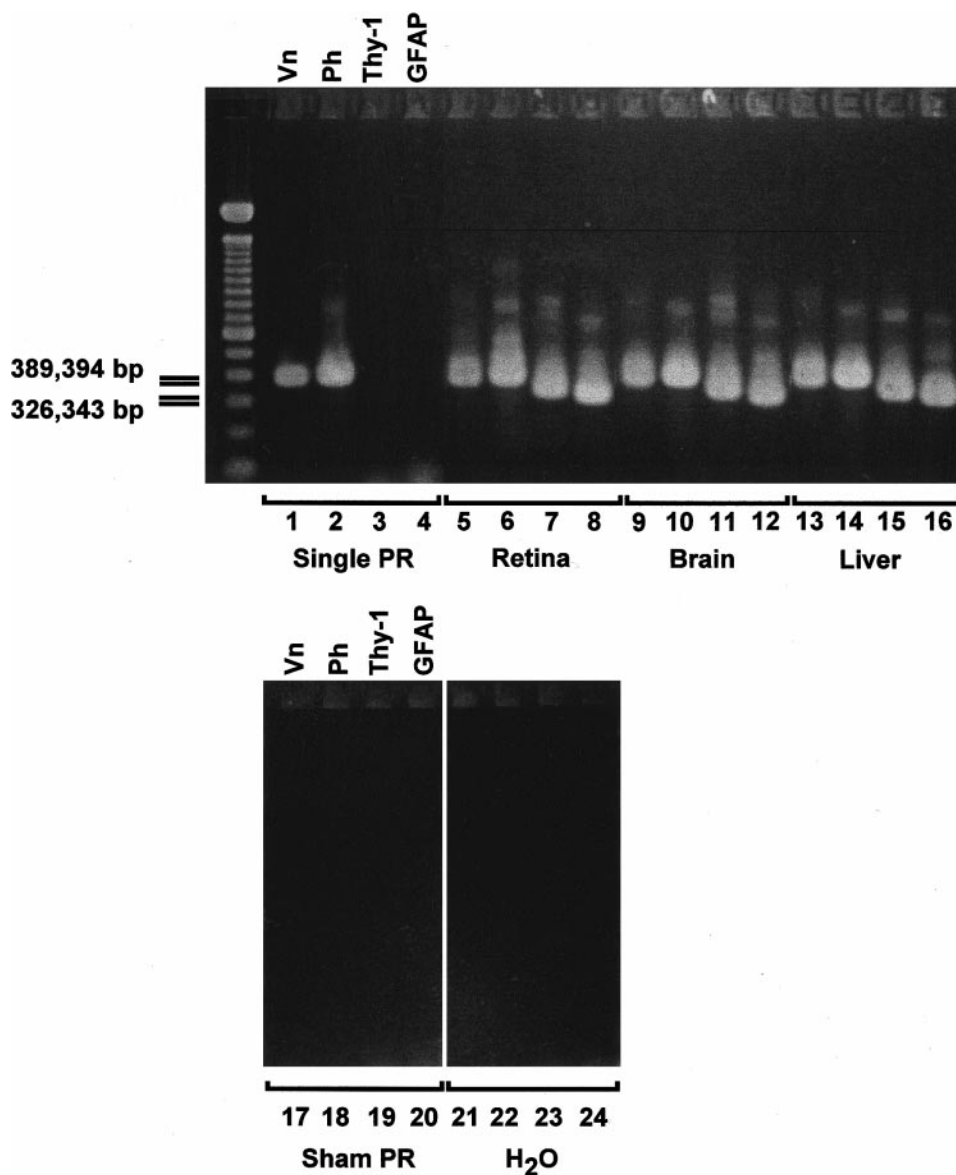


FIGURE 7. Identification of Vn amplicons in mouse photoreceptors by single cell RT-PCR. Ethidium bromide stained 1.8% agarose gels illustrating the products obtained using primers derived from nucleotide sequences of mouse genes shown in the following order: Vn, phosducin (Ph), Thy-1, and GFAP. Lanes 1 through 4: dissociated mouse photoreceptors (PR). Lane 1: 389-bp Vn fragment; lane 2: 394-bp phosducin fragment; lanes 3 and 4: no Thy-1 (343 bp) or GFAP products (326 bp) were amplified. Positive controls were produced using total RNAs isolated from mouse retina (lanes 5 through 8), brain (lanes 9 through 12), or liver (lanes 13 through 16). Products of the appropriate size were identified in each of the four tissues. Negative controls included no template (sham PR; lanes 17 through 20) and H<sub>2</sub>O (lanes 21 through 24).

corresponding evidence of Vn biosynthesis or secretion by the RPE has emerged to date. To this list of prospective candidates we can now add the photoreceptors as a potential local cellular source of the Vn that is found in drusen.

Clearly, further investigation is required to positively identify the cell type(s) responsible for the accumulation of Vn in drusen and in Bruch's membrane, to define the function(s) of Vn in the normal adult retina, to clarify the putative role of Vn in outer segment phagocytosis, and to determine whether Vn plays a significant role in the retina's response to injury, inflammation, stress, or aging.

#### Acknowledgments

The authors thank Paul Rago, Forest Olson, Wen Wu, and Matthew Nealon for their valuable technical assistance in this investigation; and Stephen Poole for his thoughtful advice and consultation on the in situ hybridization method.

#### References

- Hayman E, Pierschbacher MD, Ohgren Y, Ruoslahti E. Serum spreading factor (vitronectin) is present at the cell surface and in tissues. *Proc Natl Acad Sci USA*. 1983;80:4003-4007.
- Hageman GS, Mullins RF, Russell SR, Johnson LV, Anderson DH. Vitronectin is a constituent of ocular drusen and the vitronectin gene is expressed in human retinal pigmented epithelial cells *FASEB J*. 1999;13:477-484.
- Izumi M, Yamada KM, Hayashi M. Vitronectin exists in two structurally and functionally distinct forms in human plasma. *Biochim Biophys Acta*. 1989;990:101-108.
- Stockmann A, Hess S, Declerck P, Timpl R, Preissner KT. Multimeric vitronectin: identification and characterization of conformation-dependent self-association of the adhesive protein. *J Biol Chem*. 1993;268:22874-22882.
- Seiffert D, Smith JW. The cell adhesion domain in plasma vitronectin is cryptic. *J Biol Chem*. 1997;272:13705-13710.
- Preissner K, Seiffert D. Role of vitronectin and its receptors in haemostasis and vascular remodeling. *Thomb Res*. 1998;89:1-21.
- Tomasini BR, Mosher DF. Vitronectin. *Prog Hemost Thromb*. 1991;10:269-305.

8. Seiffert D, Keeton M, Eguchi Y, Sawdey M, Loskutoff DJ. Detection of vitronectin mRNA in tissues and cells of the mouse. *Proc Natl Acad Sci USA*. 1991;88:9402-9406.
9. Seiffert D, Podor TJ, Loskutoff DJ. Distribution of vitronectin. In: Preissner KT, Rosenblatt S, Kost C, Wegerhoff J, Mosher DF, eds. *Biology of Vitronectins and Their Receptors*. Elsevier Science; 1994:75-80.
10. Seiffert D, Bordin GM, Loskutoff DJ. Evidence that extrahepatic cells express vitronectin mRNA at rates approaching those of hepatocytes. *Histochem Cell Biol*. 1996;105:195-201.
11. Dahlback K, Loffberg H, Alumets J, Dahlback B. Immunohistochemical demonstration of age-related deposition of vitronectin (S-protein of complement) and terminal complement complex on dermal elastic fibers. *J Invest Dermatol*. 1989;92:727-733.
12. Falk R, Podack E, Dalmasso A, Jenette JC. Localization of S-protein and its relationship to the membrane attack complex of complement in renal tissue. *Am J Pathol*. 1987;127:182-190.
13. Bariety J, Hinglais N, Bhakdi S, Mandet C, Rouchon M, Kazatchkine MD. Immunohistochemical study of complement S protein (vitronectin) in normal and diseased human kidneys: relationship to neoantigens of the C5b-9 terminal complex. *Clin Exp Immunol*. 1989;75:76-81.
14. Akiyama H, Kawamata T, Dedhar S, McGeer PL. Immunohistochemical localization of vitronectin, its receptor and beta-3 integrin in Alzheimer brain tissue. *J Neuroimmunol*. 1991;32:19-28.
15. Sato R, Komine Y, Imanaka T, Takano TJ. Monoclonal antibody EMR 1a/213D recognizing site of deposition of extracellular lipid in atherosclerosis. Isolation and characterization of a cDNA clone for the antigen. *J Biol Chem*. 1990;265:21232-21236.
16. Niculescu F, Rus HG, Porutiu D, Ghiurca V, Vlaicu R. Immunoelectron-microscopic localization of S-protein/vitronectin in human atherosclerotic wall. *Atherosclerosis*. 1989;78:197-203.
17. Guettier C, Hinglais N, Bruneval P, Kazatchkine M, Bariety J, Camilleri J-P. Immunohistochemical localization of S-protein/vitronectin in human atherosclerotic versus arteriosclerotic arteries. *Virchows Arch*. 1989;414:309-313.
18. Hayman E, Pierschbacher MD, Suzuki S, Ruoslahti E. Vitronectin: a major cell attachment promoting protein in fetal bovine serum. *Exp Cell Res*. 1985;160:245-258.
19. Geller S, Lewis GP, Anderson DH, Fisher SK. Use of the MIB-1 antibody for detecting proliferating cells in the retina. *Invest Ophthalmol Vis Sci*. 1995;36:737-744.
20. Matsumoto B, Hale I. Preparation of retinas for studying photoreceptors with confocal microscopy. *Methods Neurosci*. 1993:54-71.
21. Abe T, Kikuchi T, Chang T, Shinohara T. The sequence of the mouse phosphatidylinositol-3-OH kinase-encoding gene and its 5'-flanking region. *Gene*. 1993;133:179-186.
22. Danner S, Lohse MJ. Phosphatidylinositol-3-OH kinase is a ubiquitous G-protein regulator. *Proc Natl Acad Sci USA*. 1996;93:10145-10150.
23. Suzuki S, Oldberg A, Hayman EG, Pierschbacher MD, Ruoslahti E. Complete amino acid sequence of human vitronectin deduced from cDNA: similarity of cell attachment sites in vitronectin and fibronectin. *EMBO J*. 1985;4:2519-2524.
24. Seki T, Chang HC, Moriuchi T, Denome R, Ploegh H, Silver J. A hydrophobic transmembrane segment at the carboxyl terminus of thy-1. *Science*. 1985;227:649-651.
25. Mahanthappa N, Patterson PH. Thy-1 involvement in neurite outgrowth: perturbation by antibodies, phospholipase C, and mutation. *Neurosci Lett*. 1992;137:75-77.
26. Petersen B, Goff JP, Greenberger JS, Michalopoulos GK. Hepatic oval cells express the hematopoietic stem cell marker Thy-1 in the rat. *Hepatology*. 1998;27:433-445.
27. Balcarek J, Cowan NJ. Structure of the mouse glial fibrillary acidic protein gene: implications for the evolution of the intermediate filament multigene family. *Nucleic Acids Res*. 1985;13:5527-5543.
28. Neugebauer K, Emmett CJ, Ventstrom KA, Reichardt LF. Vitronectin and thrombospondin promote retinal neurite outgrowth: developmental regulation and role of integrins. *Neuron*. 1991;6:345-358.
29. Ozaki S, Johnson LV, Mullins RF, Hageman GS, Anderson DH. The human retina and retinal pigment epithelium are abundant sources of vitronectin mRNA. *Biochem Biophys Res Commun*. 1999;258:524-529.
30. Sobel R, Chen M, Maeda A, Hinojosa JR. Vitronectin and integrin vitronectin receptor localization in multiple sclerosis lesions. *J Neuropathol Exp Neurol*. 1995;54:202-213.
31. Blancher C, Boubaker O, Bidou Laure Pessac B, Crisanti P. Nectinepsin: a new extracellular matrix protein of the pexin family: characterization of a novel cDNA encoding a protein with an RGD cell binding motif. *J Biol Chem*. 1996;271:26220-26226.
32. Davis A, Hunt RC. Transferrin is made and bound by photoreceptor cells. *J Cell Physiol*. 1993;156:280-285.
33. Hammes H-P, Weiss A, Hess S, et al. Modification of vitronectin by advanced glycation alters functional properties in vitro and in the diabetic retina. *Lab Invest*. 1996;75:325-338.
34. Chen W, Lu H, Dutt K, Smith A, Hunt DM, Hunt RC. Expression of the protective proteins hemopexin and haptoglobin by cells of the neural retina. *Exp Eye Res*. 1998;67:83-93.
35. Ciambrone G, McKeown-Longo PJ. Plasminogen activator inhibitor type I stabilizes vitronectin-dependent adhesions in HT-1080 cells. *J Cell Biol*. 1990;111:2183-2195.
36. Podack E, Preissner KT, Muller Eberhard HJ. Inhibition of C9 polymerisation within the SC5b-9 complex of complement by S-protein. *Acta Pathol Microbiol Immunol Scand Suppl*. 1984;284:889-896.
37. Perry D, Wisniewski P, Daugherty GL, Downing J, Martin WJ II. Nonimmune phagocytosis of liposomes by rat alveolar macrophages is enhanced by vitronectin and is vitronectin receptor-mediated. *Am J Respir Cell Mol Biol*. 1997;17:462-470.
38. Weaver T, Hall CL, Kachel DL, et al. Assessment of in vivo attachment/phagocytosis by alveolar macrophages. *J Immunol Methods*. 1996;17:462-470.
39. Savill J, Dransfield I, Hogg N, Haslett C. Vitronectin-mediated phagocytosis of cells undergoing apoptosis. *Nature*. 1990;343:170-173.
40. Bok D. The retinal pigment epithelium: a versatile partner in vision. *J Cell Sci*. 1993;17(suppl):189-195.
41. Boyle D, Tien LF, Cooper NG, Shepherd V, McLaughlin BJ. A mannose receptor is involved in retinal phagocytosis. *Invest Ophthalmol Vis Sci*. 1991;32:1464-1470.
42. Ryeom SW, Sparrow JR, Silverstein RL. CD36 participates in the phagocytosis of rod outer segments by retinal pigment epithelium. *J Cell Sci*. 1996;109:387-395.
43. Anderson D, Johnson LV, Hageman GS. Vitronectin receptor expression and distribution at the photoreceptor-retinal pigment epithelial interface. *J Comp Neurol*. 1995;360:1-16.
44. Lin H, Clegg DO. Integrin alpha v beta 5 mediates the phagocytosis of photoreceptor rod outer segments by human retinal pigment epithelium. *Invest Ophthalmol Vis Sci*. 1998;39:1703-1712.
45. Miceli MV, Newsome DA and Tate DJ Jr. Vitronectin is responsible for serum-stimulated uptake of rod outer segments by cultured retinal pigment epithelial cells. *Invest Ophthalmol Vis Sci*. 1997;38:1588-97.
46. Finnemann S, Bonilha VL, Marmorstein AD, Rodriguez-Boulan E. Phagocytosis of rod outer segments by retinal pigment epithelial cells requires alpha v beta 5 integrin for binding but not for internalization. *Proc Natl Acad Sci USA*. 1997;94:12932-12937.
47. Peyman G, Bok D. Peroxidase diffusion in the normal and laser-coagulated primate retina. *Invest Ophthalmol*. 1972;11:35-45.
48. Sawa H, Sobel BE, Fujii S. Potentiation by hypercholesterolemia of the induction of aortic intramural synthesis of plasminogen activator inhibitor type 1 by endothelial injury. *Circ Res*. 1993;73:671-680.
49. Vinos SA, Kuchle M, Derevjaniuk NL. Blood-retinal barrier breakdown in retinitis pigmentosa: light and electron microscopic immunolocalization. *Histol Histopathol*. 1995;10:913-923.
50. Volker W, Hess S, Vischer P, Preissner KT. Binding and processing of multimeric vitronectin by vascular endothelial cells. *J Histochem Cytochem*. 1993;41:1823-832.
51. van Aken BE, Seiffert D, Thinnis T, Loskutoff DJ. Localization of vitronectin in the normal and atherosclerotic human vessel wall. *Histochem Cell Biol*. 1997;107:313-320.